Journal of Sound and Vibration (1998) **210**(3), 367–374

THE INFLUENCE OF REFRACTION AND TURBULENCE ON RAILROAD NOISE

R. MAKAREWICZ*

Kyushu Institute of Design, 9-1 *Shiobaru* 4-*chome*, *Minami-ku*, *Fukuoka*, 815 *Japan*

(*Received* 10 *June* 1997, *and in final form* 8 *October* 1997)

Turbulence caused by train motion, heat radiation and wind eddies destroys the coherent nature of the ground effect. Due to upward refraction, only a certain segment of the track contributes to noise emission. Thus, geometrical spreading and refraction govern the process of noise propagation. Noise generation is modelled by a line source of point sources with dipole directivity.

1. INTRODUCTION

It is assumed in this study that the coherent nature of the ground effect is destroyed by atmospheric turbulence [1–3]. Turbulence is generated by the motion of the train, heat radiation of the ground surface and wind eddies. It is also assumed that due to upward refraction (sunny weather), noise is heard at the receiver, O, when the train is inside a closed curve, $R(\Phi)$ (see Figure 1), and that the train is moving along a straight line at the perpendicular distance, D, from the receiver. In such a case, the sound exposure, E, depends on the length of the track segment, AB, which contributes to the noise reaching the receiver. The increase of the perpendicular distance, D, decreases the length of AB, which is a function of refraction, and diminishes the sound exposure, E. Thus, there are two mechanisms of noise attenuation: geometrical spreading and refraction.

A rigorous solution of the problem of sound propagation in a refractive and turbulent atmosphere is both numerically and experimentally difficult [4]. Therefore, it is attempted here to construct a model of train noise simple enough, yet based on fundamental features of wave phenomena, similar to the models described in references [5–7].

If N trains of the same category pass the receiver during the time period T, then the time-averaged sound level is

$$L_{AT} = 10 \log \left\{ \frac{t_0}{T} \sum_{i=1}^{N} e_i \right\}, \qquad t_0 = 1 \text{ s}, \tag{1}$$

where

$$e_i = E_i / p_0^2 t_0, \qquad p_0 = 20 \ \mu\text{Pa}, \tag{2}$$

is the relative sound exposure for the ith train. Due to differences among the cars, the varying number of cars of a single train (train length), and to different speeds of trains, the process of noise generation is random. The same characteristic applies to the process of noise propagation. Due to weather variation, the shape of the curve, $R(\Phi)$, and the

* On leave from: Institute of Acoustics, A. Mickiewicz University, 60-769 Poznan, Matejki 48, Poland.

0022–460X/98/080367 + 08 $25.00/0/sv971339

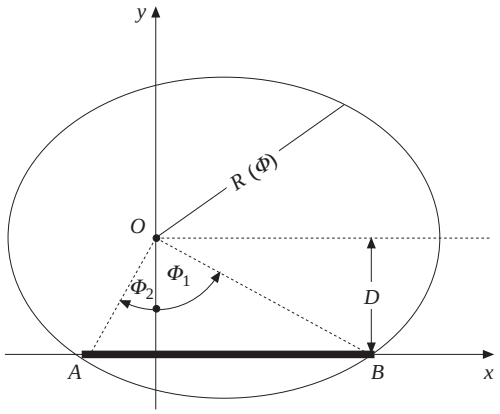

Figure 1. The segment of the track, AB, that participates in the noise emission.

length of the noise-producing track segment, AB, are varying (see Figure 1). All of the features mentioned above explain the random nature of the relative sound exposure, e_i.

When turbulence destroys the interference between the direct and reflected waves, the only result of the ground effect is the change of the sound power: $P_A^* \rightarrow \beta P_A^*$. Thus, β can be seen as a measure of the ground effect. The train noise generation is modelled by a line source of incoherent point sources with dipole directivity [8–10]. Thus, the A-weighted squared sound pressure due to geometrical spreading from the line source of unit length, $l_0 = 1$ m, is given by

$$p_A^2 = \frac{3}{4\pi} \frac{\beta W_A^* l_0 \rho c}{d^2} \cos^2 \Phi, \tag{3}$$

where W_A^* expresses the density of the A-weighted sound power in watts per meter, ρc is the characteristic impedance of air, d denotes the horizontal distance, and the angle $\Phi = \cos^{-1}(D/d)$ lies in the x–y plane (see Figure 2). The above equation holds true for nearly grazing propagation ($\Psi \rightarrow 0$; Figure 3), with the heights of the receiver, z, and the source, H, significantly less than the horizontal distance, d:

$$z + H \ll d. \tag{4}$$

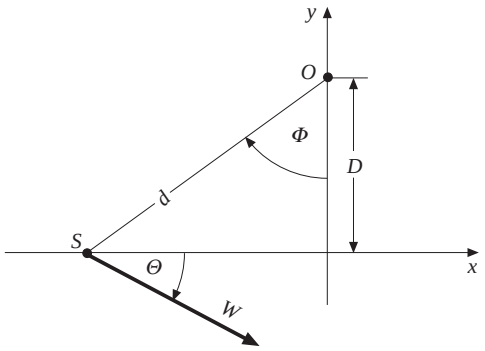

Figure 2. The momentary location of the point source, S, is determined by the perpendicular distance, D, and the angle, $\Phi > 0$.

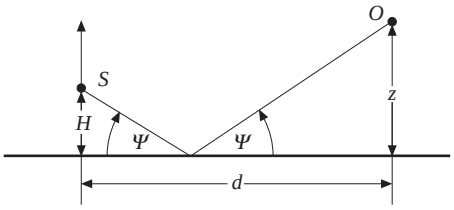

Figure 3. The unit length line source, S, and receiver, O, are at the heights, H, and z, respectively.

Without refraction, i.e., with $R(\Phi) = \infty$ for each ray $0 \leqslant \Phi < 2\pi$, all points of the track contribute to the noise at the receiver, O, so the sound exposure, E, is defined by the integral between the limits $\Phi_1 = -\pi/2$ and $\Phi_2 = +\pi/2$ [10, 11],

$$E = \frac{Dl}{Vl_0} \int_{-\pi/2}^{+\pi/2} \frac{p_A^2(\Phi)}{\cos^2 \Phi} \, \mathrm{d}\Phi, \tag{5}$$

where l is the train length and V denotes its speed. This equation can be used when the rays are bending downward (night) and the shadow zone disappears.

In section 2 it is shown that the upward refraction (day) changes the limits of integration in the above equation. In section 3 the formula for the time-averaged sound level is derived. Next, the effect of turbulence is considered (section 4).

2. REFRACTION

It is assumed that the atmosphere is stratified, so the sound speed, c, and the wind speed, W, are both functions of the altitude, z. In the presence of wind, as is shown in Figure 2, noise undergoes refraction as if it were propagating in the atmosphere at rest, but with the effective sound speed [12] (see Figure 2)

$$\tilde{c} = c(z) + W(z) \sin(\Phi - \Theta), \tag{6}$$

where the angle Θ determines the wind direction. Linear approximation of the sound speed

$$c(z) = c(0)(1 - \zeta z), \tag{7}$$

with ζ expressing the sound speed gradient, explains some field data quite satisfactorily[13–15]. Introducing the wind speed gradient, η, one can write

$$W(z) = c(0)\eta z, \tag{8}$$

and obtain the effective sound speed as a linear function of the altitude, z:

$$\tilde{c}(z) = c(0)\{1 - [\zeta - \eta \sin(\Phi - \Theta)z]\}. \tag{9}$$

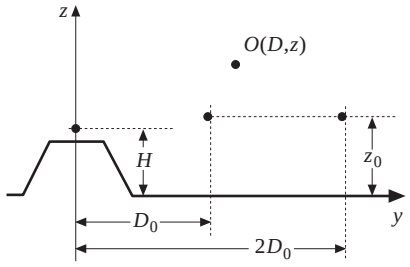

Figure 4. Measurements of the sound exposure level, L_{AE}, at the perpendicular distances, D_0 and $2D_0$, with microphones at the height z_0.

Train noise reaches the receiver, O, when each car of the train is inside the closed curve [16, 17],

$$R(\Phi) = R_0[1 - \chi \sin(\Phi - \Theta)]^{-1/2}, \tag{10}$$

where the circle's radius

$$R_0 = (\sqrt{z} + \sqrt{H})/\xi, \tag{11}$$

yields the distance to the shadow zone in a calm atmosphere, $\eta = 0$, which is induced only by the sound speed gradient, ζ. Due to turbulence, the variables

$$\chi = \eta/\zeta \qquad \text{and} \qquad \xi = (\zeta/2)^{1/2}, \tag{12}$$

are random. They may be different during each pass-by of a train: i.e., the shape of the curve $R(\Phi)$ (equation (10)) varies over time. For example, taking $\eta = 0$ and $\zeta = 2 \times 10^{-4}$ [1/m], with $H = 0$ and $z = 1$ m, one obtains a circle of radius, $R_0 = 100$ m.

The angles Φ_1 and Φ_2, which determine the track segment AB, are the solutions to the equation (see Figure 1)

$$R(\Phi)\cos\Phi = D. \tag{13}$$

For a weak wind, $\eta \ll \zeta$, i.e., $\chi \ll 1$ (equation (12)), the combination of equations (10) and (13) yields

$$\sin\Phi_1 \approx -\cos^{-1}(n\xi), \tag{14}$$

and

$$\sin\Phi_2 \approx +\cos^{-1}(n\xi),$$

where the parameter

$$n = D/(\sqrt{z} + \sqrt{H}) \tag{15}$$

is constant and fully determined by the track–receiver geometry. It is assumed that random variations of ξ are caused by turbulence (see section 4).

3. TIME-AVERAGED SOUND LEVEL

By changing the limits of integration equation (5), $(-\pi/2)\to\Phi_1$ and $(+\pi/2)\to\Phi_2$, one obtains from equation (2) the relative sound exposure that accounts for refraction,

$$e = \frac{3}{4\pi}\frac{l_0}{D}\mu J, \tag{16}$$

where

$$J = \int_{\Phi_1(\xi)}^{\Phi_2(\xi)} \cos^2\Phi \, \mathrm{d}\Phi. \tag{17}$$

Fluctuations of the angles Φ_1 and Φ_2, which describe the process of noise propagation, lead to variations of the relative sound exposure, e. The random process of noise generation is quantified by

$$\mu = \beta \frac{W_A^* l}{V} \Big/ \frac{P_0}{V_0}, \tag{18}$$

with the reference sound power, $P_0 = 10^{-12}$ W and the speed unit, $V_0 = l_0/t_0$. The product $W_A^* l$ (in watts) is the A-weighted sound power of the whole train of length, l. Because the dimensions of both $W_A^* l/V$ and P_0/V_0, are joules per meter, μ represents the relative density of the sound power.

The variables μ and ξ fluctuate about their means; hence, for the ith train one can write

$$\mu_i = \bar{\mu} + \delta\mu_i, \qquad \xi_i = \overline{\xi} + \delta\xi_i. \tag{19}$$

Consequently, equation (16) can be rewritten as

$$e_i = e(\bar{\mu}, \overline{\xi}) F(\delta\mu_i, \delta\xi_i), \tag{20}$$

where the relative sound exposure, e, for the average μ, and ξ, is

$$e(\bar{\mu}, \overline{\xi}) = \frac{3}{4\pi} \frac{l_0}{D} \bar{\mu} \int_{\Phi_1(\overline{\xi})}^{\Phi_2(\overline{\xi})} \cos^2 \Phi \, \mathrm{d}\Phi. \tag{21}$$

The explicit form of the weather factor, $F(\ldots)$, will be derived in the next section. Introducing the average weather factor,

$$\langle F \rangle = \frac{1}{N} \sum_{i=1}^{N} F(\delta\mu_i, \delta\xi_i), \tag{22}$$

one arrives at the time-averaged sound level (equation (1))

$$L_{AT} = 10 \log \{N t_0/T\} + \tilde{L}_{AE}, \tag{23}$$

where the sound exposure level is

$$\tilde{L}_{AE} = 10 \log \{e(\bar{\mu}, \overline{\xi}) \langle F \rangle\}. \tag{24}$$

4. TURBULENCE

For the atmosphere at rest, the shadow zone is determined by a circle of radius R_0 with constant value of ξ (equation (11)). The variations of the wind speed, its direction, the temperature eddies, and the turbulence generated by the motion of the train, however, result in fluctuations of the variable ξ, so that the radius R_0 fluctuates as well. Substituting Φ_1 and Φ_2 into equation (17) gives the relative sound exposure (equation (16))

$$e_i = \frac{3}{4\pi} \frac{l_0}{D} \mu_i [\cos^{-1}(n\xi_i) + n\xi_i \sqrt{1 - (n\xi_i)^2}]. \tag{25}$$

When the fluctuations of ξ_i are small, $|\delta\xi_i/\overline{\xi}| < 1$, one can rewrite expression (25) in the form given by equation (20), where the weather factor is defined by

$$F_i \approx \left[1 + \frac{\delta\mu_i}{\bar{\mu}}\right]\left[1 + G_1(n\overline{\xi}) \frac{\delta\xi_i}{\overline{\xi}} + G_2(n\overline{\xi})\left(\frac{\delta\xi_i}{\overline{\xi}}\right)^2\right]. \tag{26}$$

For $n\overline{\xi} < 1$ (equations (11), (12) and (15)—the train beyond the shadow zone) the functions G_1 and G_2 are

$$G_1 = -2(n\overline{\xi})^3/[1 - (n\overline{\xi})^2]^{1/2}[\cos^{-1}(n\overline{\xi}) + n\overline{\xi}\sqrt{1 - (n\overline{\xi})^2}]$$

and

$$G_2 = (n\overline{\xi})^3[(n\overline{\xi})^2 - 2]/[1 - (n\overline{\xi})^2]^{3/2}[\cos^{-1}(n\overline{\xi}) + n\overline{\xi}\sqrt{1 - (n\overline{\xi})^2}]. \tag{27}$$

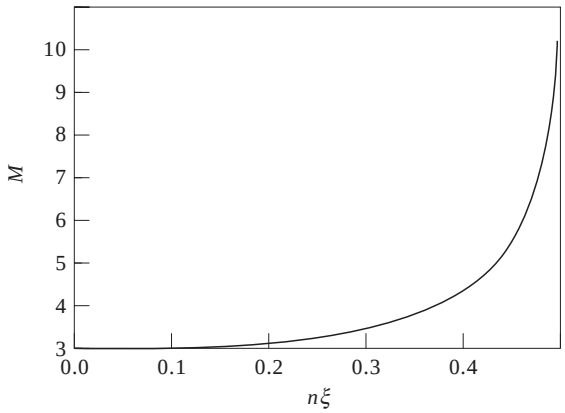

Figure 5. The dependence of M (equation (32)) on the product, $n\xi$ (equations (12) and (15)).

Finally, equations (22) and (26) yield the average weather factor

$$\langle F \rangle = 1 + G_1 m_{\mu\xi} + G_2 m_{\xi\xi}, \tag{28}$$

where the statistical moments are

$$m_{\xi\xi} = \frac{1}{N}\sum_{i=1}^{N}\left(1 - \frac{\xi_i}{\bar{\xi}}\right)^2 \qquad \text{and} \qquad m_{\mu\xi} = \frac{1}{N}\sum_{i=1}^{N}\left(1 - \frac{\mu_i}{\bar{\mu}}\right)\left(1 - \frac{\xi_i}{\bar{\xi}}\right). \tag{29}$$

The combination of equations (23)–(25) and (28) gives the time-averaged sound level, L_{AT}.

To find the numerical value of L_{AT}, the averages, $\bar{\mu}$ and $\bar{\xi}$, and the moments, $m_{\mu\xi}$ and $m_{\xi\xi}$, must first be determined. The variables μ_i and ξ_i for each train can be determined from two simultaneous measurements of the sound exposure level

$$L_{AE} = 10 \log \{e\}, \tag{30}$$

performed at perpendicular distances, D_0 and $2D_0$, with the same height, $z = z_0$ (see Figure 4). From equations (25) and (30) one obtains the relationship

$$M(n\xi) = L_{AE}^{(i)}(D_0) - L_{AE}^{(i)}(2D_0), \tag{31}$$

where the function

$$M(n\xi) = 10 \log \left\{ \frac{\cos^{-1}(n\xi) + n\xi\sqrt{1 - (n\xi)^2}}{\cos^{-1}(2n\xi) + 2n\xi\sqrt{1 - (2n\xi)^2}} \right\} + 3 \text{ dB}, \tag{32}$$

is plotted in Figure 5. Entering the abscissa with the difference of the sound exposure levels (right side of equation (31)), one obtains the corresponding value of $n\xi$. Then, with equation (15), the value of ξ is available. Finally, for the given $n\xi$, D_0, and $L_{AE}(D_0)$, the relative density of sound power can be calculated (equations (25) and (30)):

$$\mu = 10^{L_{AE}(D_0)/10}(4\pi D_0/3l_0)[\cos^{-1}(n\xi) + n\xi\sqrt{1 - (n\xi)^2}]^{-1}. \tag{33}$$

4.1. EXPERIMENT

Noise was produced by a commuter train, Fukuoka–Omuta (Japan), moving with a steady speed on an embankment of height $H \approx 1$ m, between 9 p.m. and 1 a.m. The weather was fair with a partly cloudy sky. The terrain was open, without buildings or any other reflecting objects nearby. The wind direction was changing, with the average speed about 2 m/s. Simultaneous measurements of $L_{AE}(D_0)$ and $L_{AE}(2D_0)$ at the distance,

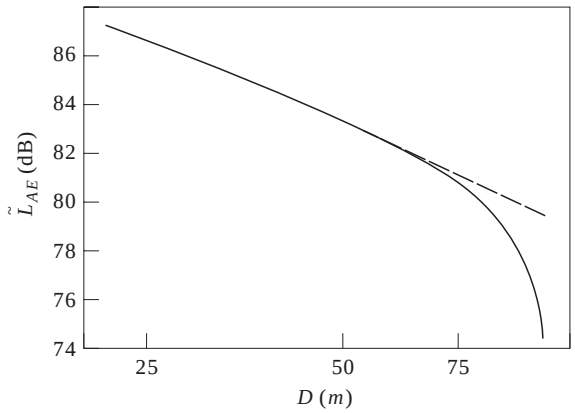

Figure 6. The theoretical prediction of the sound exposure level, $\tilde{L}_{AE}$ (equation (34)) for the height, $z = 1$ m. — —, 3 dB decrease per doubling of distance.

$D_0 = 50$ m and $2D_0 = 100$ m, with microphones at the heights, $z_0 = 1$ m, were performed (see Figure 4). Then, for each train the variables ξ_i and μ_i (equations (32) and (33); see Figure 5), were determined and their averages, $\bar{\xi}$ and $\bar{\mu}$, and moments $m_{\mu\xi}$ and $m_{\xi\xi}$ (equations (29)) were calculated. For ten trains the results are as follows: $\bar{\xi} = 0{\cdot}0195$, $\bar{\mu} = 3{\cdot}03 \times 10^{10}$, $m_{\xi\xi} = 3{\cdot}14 \times 10^{-4}$ and $m_{\mu\xi} = -1{\cdot}44 \times 10^{-3}$.

For the site in question, the sound exposure level, $\tilde{L}_{AE}$ (equations (24), (25) and (28)) depends on the height of the receiver, z, and its perpendicular distance from the track, D:

$$\tilde{L}_{AE}(D, z) \approx 98{\cdot}6 + 10 \log \{(l_0/D) f(D, z)\}, \tag{34}$$

where

$$f(D, z) = \cos^{-1}(q) + q\sqrt{1 - q^2} + 2{\cdot}88 \times 10^{-3} \frac{q^3}{[1 + q^2]^{1/2}} + 2{\cdot}00 \times 10^{-4} \frac{q^3[q^2 - 2]}{[1 - q^2]^{3/2}}, \tag{35}$$

and

$$q = 10^{-2}\, 1{\cdot}95D/(\sqrt{z} + 1). \tag{36}$$

Setting $\bar{\xi} = 0{\cdot}0195$ into equation (11) one obtains the distance to the shadow zone, i.e., the radius of the circle

$$R_0 = 51{\cdot}3(\sqrt{z} + 1). \tag{37}$$

For the receiver height, $z = 1$ m, equation (37) yields $R_0 = 103$ m. In Figure 6 is shown the sharp decline of $\tilde{L}_{AE}(D, z = 1)$ calculated from equation (34), when the perpendicular distance, D, approaches $R_0 = 103$ m.

5. CONCLUSIONS

A model of train noise has been derived under the following assumptions: noise is generated by a line source of point sources with dipole directivity; coherent interaction of the direct and reflected waves is extinguished by turbulence, so geometrical spreading and refraction are the predominant wave phenomena; the wind speed gradient, η, is much less than the sound speed gradient, ζ; the receiver is located beyond the shadow zone.

For a weak wind, with the speed gradient, η (equation (8)) significantly less than the sound speed gradient ζ (equation (7)), the sound exposure level, $\tilde{L}_{AE}(D, z)$, and the time-averaged sound level, $L_{AT}(D, z)$, can be predicted from equations (23)–(25), (27) and

(28). To estimate the values of $\bar{\mu}$, $\bar{\xi}$, $m_{\mu\xi}$ and $m_{\xi\xi}$, simultaneous measurements of the sound exposure level $L_{AE}(D_0)$ and $L_{AE}(2D_0)$ have to be performed at distances D_0 and $2D_0$ (see Figure 4).

To validate the model, at the height $z = 1$ m and the perpendicular distance $D = 25$ m from the track, measurements were obtained over a 2 hour period (sunny day), yielding the time-averaged sound level $L_{A2} = 60{\cdot}4$ dB. Noise was generated by ten trains that passed the microphone during the time interal, $T = 7200$ s, while the wind was blowing perpendicular to the track with the average speed about 2 m/s. For $D = 25$ m and $z = 1$ m, a theoretical prediction of the sound exposure level is given in Figure 6: $\tilde{L}_{AE} = 86{\cdot}6$ dB. Taking $N = 10$ and $T = 7200$ s, one obtains $L_{AT} = 58{\cdot}0$ dB (equation (23)). The difference between the theoretical value and the experimental result was 2·4 dB. This is a significant difference, so the theory must be refined. Certainly, the wind direction plays some role. Additionally, geometrical spreading and refraction are not the only phenomena that govern noise propagation during windy weather.

ACKNOWLEDGMENTS

The author thanks Mr M. Yoshida for technical assistance and the anonymous reviewers for their valuable comments.

REFERENCES

1. J. E. Piercy, T. F. W. Embleton and L. C. Sutherland 1977 *Journal of the Acoustical Society of America* **61**, 1403–1418. Review of noise propagation in the atmosphere. (See Figure 16).
2. K. Yamamoto and M. Yamashita 1994 *Journal of the Acoustical Society of Japan* (*E*) **15**, 1–12. Measurements and analysis of sound propagation over lawn. (See Figure 3.)
3. T. F. W. Embleton 1996 *Journal of the Acoustical Society of America* **100**, 31–48. Tutorial on sound propagation outdoors (See Figure 18.)
4. P. Chevret, Ph. Blanc-Benon and D. Juve 1996 *Journal of the Acoustical Society of America* **100**, 3587–3599. A numerical model for sound propagation through a turbulent atmosphere near the ground.
5. P. M. Nelson (editor) 1987 *Transportation Noise Reference Book*. London: Butterworths.
6. C. H. Harris (editor) 1991 *Acoustical Measurements and Noise Control*. New York: McGraw-Hill.
7. L. L. Beranek and I. L. Ver (editors) 1992 *Noise and Vibration Control Engineering*. New York: John Wiley.
8. B. Hemsworth 1987 in *Transportation Noise Reference Book* (P. M. Nelson, editor). London: Butterworths. Prediction of train noise.
9. D. Hohenwarter 1990 *Journal of Sound and Vibration* **141**, 17–41. Railway noise propagation models.
10. R. Makarewicz, K. B. Rasmussen and P. Kokowski 1996 *Acustica* **82**, 636–641. Ground attenuation of railroad noise.
11. R. Makarewicz and M. Yoshida 1996 *Applied Acoustics* **49**, 291–306. Railroad noise in an open space.
12. A. D. Pierce 1981 *Acoustics*. New York: McGraw-Hill.
13. T. Hidaka, K. Kageyama and S. Masuda 1985 *Journal of the Acoustical Society of Japan* (*E*) **6**, 117–125. Sound propagation in the rest atmosphere with linear sound velocity profile.
14. A. L'Esperance, P. Herzog, G. A. Daigle and J. R. Nicolas 1992 *Applied Acoustics* **37**, 1403–1428. Heuristic model for outdoor sound propagation based on the geometrical ray theory in the case of a linear sound profile.
15. K. B. Rasmussen 1986 *Journal of Sound and Vibration* **104**, 321–335. Outdoor sound propagation under the influence of wind and temperature gradient.
16. F. M. Wiener and D. N. Keast 1959 *Journal of the Acoustical Society of America* **31**, 724–733. Experimental study of the propagation of sound over ground.
17. R. Makarewicz 1989 *Journal of the Acoustical Society of America* **85**, 1092–1096. The shadow zone in stratified media.